International Research Journal of Engineering and Technology (IRJET) e-ISSN: 2395 -0056
Volume: 04 Issue: 05 | May -2017 www.irjet.net p-ISSN: 2395-0072

A New Topology of Transformerless Inverter for BLDC Drive System Using PV Applications

OLETI HIMA KIRAN KUMAR[1], KANAPRATHI RAVI KUMAR[2], MERAJOTU PRATAP NAIK[3]

[1,2,3]*Assistant Professor, Department of Electrical & Electronics Engineering, KKR & KSR Institute of Technology and Sciences, Vinjanampadu, Guntur (Dt), Andhra Pradesh*

Abstract - *Utility applications and large electric drives require modern power electronics converters to meet the high power demands. As a result, an alternative for medium voltage and high power applications is done by introducing structure of power converter using Renewable energy sources (RES). RES play an important role in rural areas where the power transmission from conventional energy sources is difficult. Other advantages of renewable energy sources are clean, light and does not pollute atmosphere. In order to meet the required load demand, it is better to integrate the renewable energy sources with the application of drive connected scheme by using inverter module. In these conditions, dangerous leakage currents (common-mode currents) can appear through the stray capacitance between the PV array and the ground. The former, in order to create a galvanic isolation between the input and the output include a transformer that limits the whole system performances in terms of efficiency, weight, size and cost. On the contrary, transformerless inverters do not present any isolation and are characterized by little size, lower cost and higher efficiency (more than 2% higher). In this paper presents a high-reliability single-phase transformerless grid-connected inverter that operate super junction MOSFETs to accomplish high efficiency for photovoltaic applications. In this paper proposed converter tested for the BLDC drive system is applied and it is analyzed*

***Key Words*: BLDC Motor, PV Systems transformer less inverter,**

1.INTRODUCTION

Nowadays, photovoltaic (PV) energy has attracted interest as a next generation energy source capable of solving the problems of global warming and energy exhaustion caused by increasing energy consumption. PV energy avoids unnecessary fuel expenses and there is no air pollution or waste. Also, there are no mechanical vibrations or noises because the components of power generation based on PV energy use semiconductors. The life cycle of the solar cell is more than 20 years, and it can minimize maintenance and management expenses. The output power of the solar cell is easily changed by the surrounding conditions such as irradiation and temperature, and also its efficiency is low. Thus high efficiency is required for the power conditioning system (PCS), which transmits power from the PV array to the load. In general, a single-phase PV PCS consists of two conversion stages (i.e., dc/dc conversion stage and dc/ac conversion stage). The dc/dc converter is the first stage and it performs maximum power-point tracking (MPPT) and Guarantees the dc-link voltage under low irradiance conditions [1]. Power electronic converters, especially dc/ac PWM inverters have been extending their range of use in industry because they provide reduced energy consumption, better system efficiency, improved quality of product, good maintenance, and so on [2]-[4]. Based on the high voltage gain conversion topology is fed to BLDC drive to update the characteristics of proposed conversion scheme for many residential applications. Brushless DC motors with trapezoidal Back-EMF have several inherent advantages. Most prominent among them are high efficiency and high power density due to the absence of field winding, in addition the absence of brushes leads to high reliability, low maintenance and high capability High frequency common-mode (CM) voltages must be avoided for a transformerless PV grid-connected inverter because it will lead to a large charge/discharge current partially flowing through the inverter to the ground. This CM ground current will cause an increase in the current harmonics, higher losses, safety problems, and electromagnetic interference (EMI) issues. The reported system peak and CEC efficiencies with an 8- kW converter system from the product datasheet is 98.3% and 98%, respectively, with 345-V dc input voltage and a 16-kHz switching frequency. However, this topology has high conduction losses due to the fact that the current must conduct through three switches in series during the active phase. Another disadvantage of the H5 is that the line-frequency switches S1 and S2 cannot utilize MOSFET devices because of the MOSFET body diode's slow reverse recovery. Replacing the switch S5 of the H5 inverter with two split switches S5 and S6 into two phase legs and adding two freewheeling diodes D5 and D6 for freewheeling current flows, the H6 topology was proposed in [12]. The H6 inverter can be implemented using MOSFETs for the line frequency switching devices, eliminating the use of less efficient IGBTs. The reported peak efficiency and EU efficiency of a 300 W prototype circuit were

98.3% and 98.1%, respectively with 180 V dc input voltage and 30 kHz switching frequency [5].

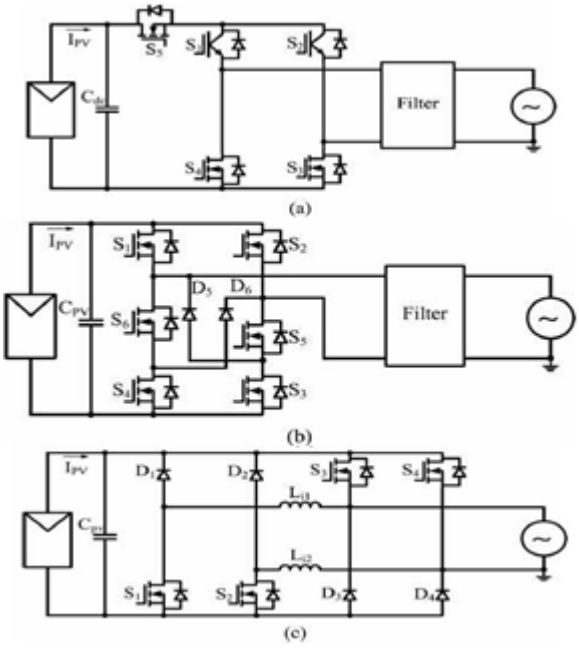

Fig. 1 Single-phase transformerless PV inverters using super junction MOSFETs: (a) H5, (b) H6, and (c) dual-paralleled-buck inverters

Another high-efficiency transformerless MOSFET inverter topology is the dual-paralleled-buck converter, as shown in Fig. 1(c). The dual-parallel-buck converter was inversely derived from the dual-boost bridgeless power-factor correction (PFC) circuit in [6]. The dual- paralleled-buck inverter eliminates the problem of high conduction losses in the H5 and H6 inverter topologies because there are only two active switches in series with the current path during active phases. This adjustment to improve the system reliability comes at the cost of high zero-crossing distortion for the output grid current. One key issue for a high efficiency and reliability transformerless PV inverter is that in order to achieve high efficiency over a wide load range it is necessary to utilize MOSFETs for all switching devices. Another key issue is that the inverter should not have any shoot-through issues for higher reliability. In order to address these two key issues, a new inverter topology is proposed for single-phase transformerless PV grid-connected systems in this paper. The proposed transformerless PV inverter features: 1) high reliability because there are no shoot-through issues, 2) low output ac current distortion as a result of no dead-time requirements at every PWM switching commutation instant as well as at grid zero-crossing instants, 3) minimized CM leakage current because there are two additional ac-side switches that decouple the PV array from the grid during the freewheeling phases. As a result of the low conduction and switching losses of the superjunction MOSFETs, the proposed converter can be designed to operate at higher switching frequencies while maintaining high system efficiency. Higher switching frequencies reduce the ac-current ripple and the size of passive components.

2 PROPOSED TOPOLOGY AND OPERATION ANALYSIS

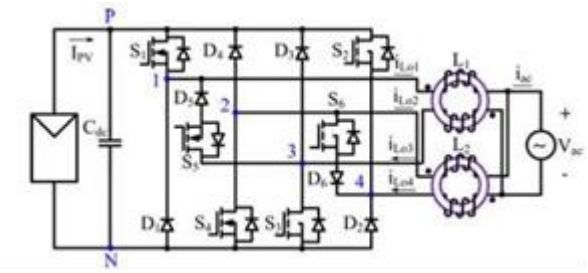

Fig.2 proposed high efficiency and reliability PV transform less inverter topology

Fig. 2 shows the circuit diagram of the proposed transformerless PV inverter, which is composed of six MOSFETs switches (S1–S6), six diodes (D1–D6), and two split ac-coupled inductors *L*1 and *L*2 . The diodesD1–D4 perform voltage clamping functions for active switches S1–S4 . The ac-side switch pairs are composed of S5, D5 and S6, D6, respectively, which provide unidirectional current flow branches during the freewheeling phases decoupling the grid from the PV array and minimizing the CM leakage current. Compared to the HERIC topology in [7]-[9] the proposed inverter topology divides the ac side into two independent units for positive and negative half cycle. In addition to the high efficiency and low leakage current features, the proposed transformerless inverter avoids shoot-through enhancing the reliability of the inverter. The inherent structure of the proposed inverter does not lead itself to the reverse recovery issues for the main power switches and as such superjunction MOSFETs can be utilized without any reliability or efficiency penalties.

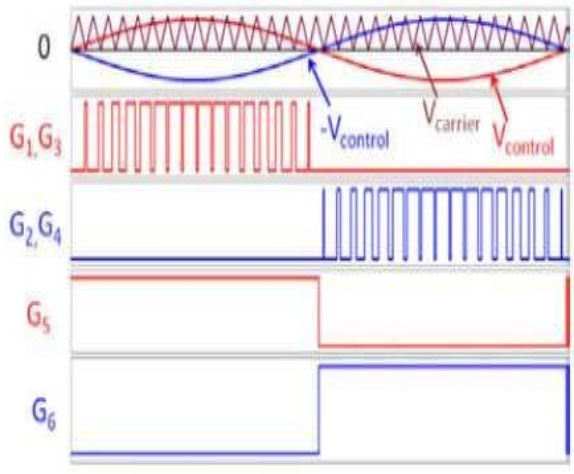

Fig. 3 Gating signals of the proposed transformerless PV inverter

Fig. 3 illustrates the PWM scheme for the proposed inverter. When the reference signal *V*control is higher than zero, MOSFETs S1 and S3 are switched simultaneously in the PWM mode and S5 is kept on as a polarity selection switch in the half grid cycle; the gating signals G2, G4 , and G6 are low and S2, S4 , and S6 are inactive. Similarly, if the reference signal – *V*control is higher than zero, MOSFETs S2 and S4 are switched simultaneously in the PWM mode and S6 is on as a polarity selection switch in the grid cycle; the gating signals G1, G3 , and G5 are low and S1, S3, and S5 are inactive.

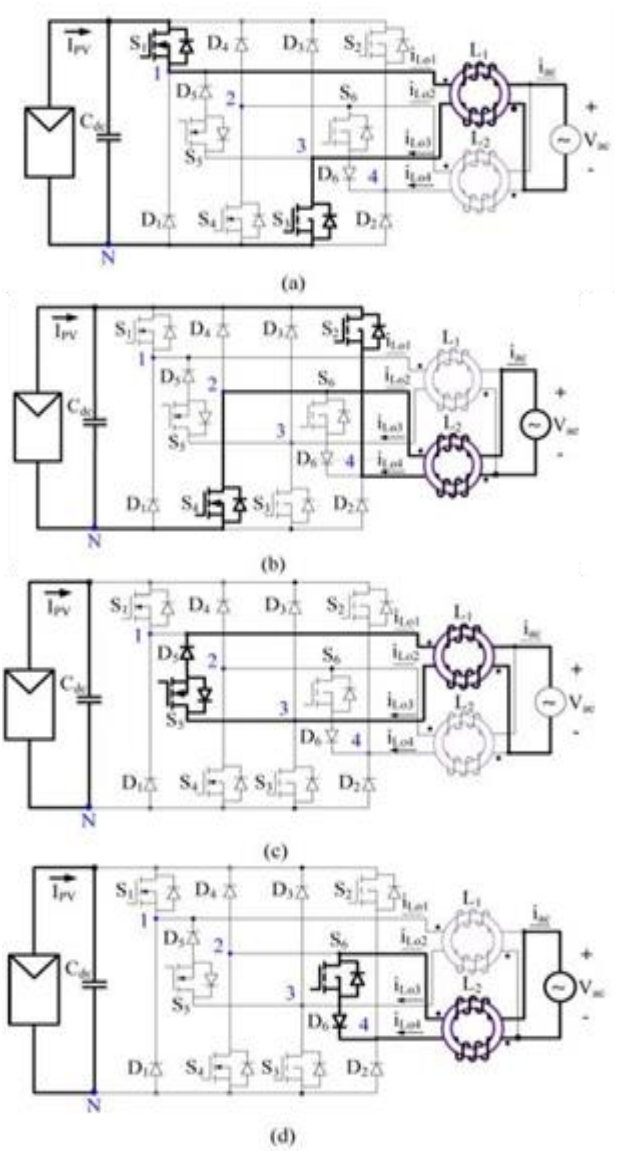

Fig.4 Topological stages of the proposed inverter :

(a) active stage of positive half-line cycle, (b) freewheeling stage of positive half-line cycle, (c) active stage of negative half-line cycle, and (d)freewheeling stage of negative half-line cycle

Fig. 4 shows the four operation stages of the proposed inverter within one grid cycle. In the positive half-line grid cycle, the high-frequency switches S1 and S3 are modulated by the sinusoidal reference signal *V*control while S5 remains turned ON. When S1 and S3 are ON, diode D5 is reverse-biased, the inductor currents of *i*Lo1 and *i*Lo3 are equally charged, and energy is transferred from the dc source to the grid; when S1 and S3 are deactivated, the switch S5 and diode D5 provide he inductor current *iL*1 and *iL*3 a freewheeling path decoupling the PV panel from the grid to avoid the CM leakage current [10]-[12]. Coupled-inductor *L*2 is inactive in the positive half-line grid cycle. Similarly, in the negative half cycle, S2 and S4 are switched at high frequency and S6 remains ON. Freewheeling occurs through S6 and D6.

3. Ground Loop Leakage Current Analysis for the Proposed Transformerless Inverter

A galvanic connection between the ground of the grid and the PV array exists in transformerless grid- connected PV systems. Large ground leakage currents may appear due to the high stray capacitance between the PV array and the ground. In order to analyze the ground loop leakage current, Fig. 5 shows a model with the phase output points 1, 2, 3, and 4 modeled as controlled voltage sources connected to the negative terminal of the dc bus (N point). Fig. 5 clearly illustrates the stray elements influencing the ground leakage current, which include: 1) the stray capacitance between PV array and ground *C*PVg; 2) stray capacitances between the inverter devices and the ground *Cg*1 – *Cg*4 ; and 3) the series impedance between the ground connection points of the inverter and the grid Z*g*. The differential-mode (DM) filter capacitor *Cx* and the CM filter components *L*CM, *CY* 1 , and *CY* 2 are also shown in the model. The value of the stray capacitances *Cg*1, *Cg*2, *Cg*3 , and *Cg*4 of MOSFETs is very low compared with that of *C*PVg , therefore the influence of these capacitors on the leakage current can be neglected. It is also noticed that the DM capacitor *Cx* does not affect the CM leakage current. Moreover, during the positive half-line cycle, switches S2, S4 , and S6 are kept deactivated; hence the controlled voltage sources *V*2*N* and *V*4*N* are equal to zero and can be removed. Consequently, a simplified CM leakage current model for the positive half-line cycle is derived as shown in Fig. 6.

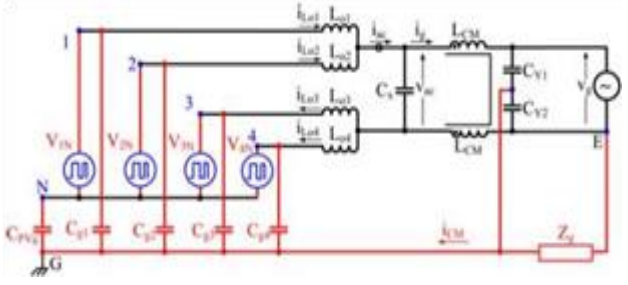

Fig.5 Leakage current analysis model for the proposed transformerless PV inverter

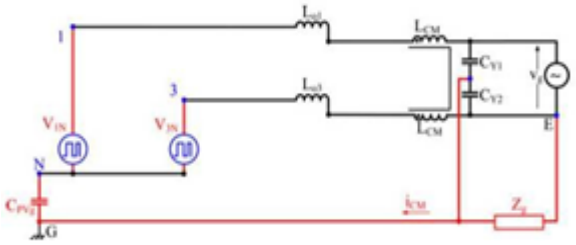

Fig. 6 Simplified CM leakage current analysis model for positive half- line cycle

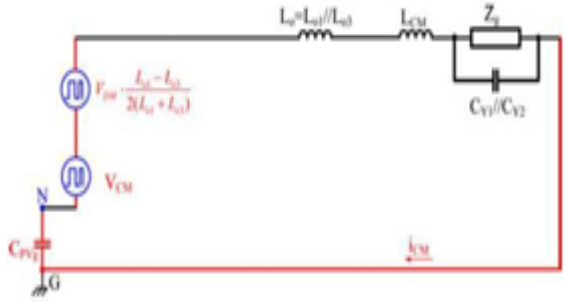

Fig.7 Simplified single-loop CM model for positive half-line cycle

With the help of the CM and DM concepts and by introducing the equivalent circuits between N and E, a single-loop mode applicable to the CM leakage current analysis for the positive half-line cycle of the proposed transformer less inverter is obtained, as shown in Fig. 7, with

$$V_{\mathrm{CM}} = \frac{V_{1N} + V_{3N}}{2} \tag{1}$$

$$V_{\mathrm{DM}} = V_{1N} - V_{3N} \tag{2}$$

A total CM voltage *Vt*CM is defined as

$$V_{t\mathrm{CM}} = V_{\mathrm{CM}} + V_{\mathrm{DM}} \cdot \frac{L_{o1} - L_{o3}}{2(L_{o1} + L_{o3})} = \frac{V_{1N} + V_{3N}}{2} + (V_{1N} - V_{3N}) \cdot \frac{L_{o1} - L_{o3}}{2(L_{o1} + L_{o3})}. \tag{3}$$

It is clear that if the total CM voltage V*t*CM keeps constant, no CM current flows through the converter. For a well-designed circuit with symmetrically structured magnetics, normally *Lo*1 is equal to *Lo*3 . During the active stage of the positive half-line cycle, *V*1*N* is equal to *V*dc, while *V*3*N* is equal to 0. Hence, the total CM voltage can be calculated as

$$V_{t\mathrm{CM}} = \frac{V_{1N} + V_{3N}}{2} + (V_{1N} - V_{3N}) \cdot \frac{L_{o1} - L_{o3}}{2(L_{o1} + L_{o3})} = \frac{V_{\mathrm{dc}}}{2}. \tag{4}$$

During the freewheeling stage of the positive half-line cycle, under the condition that S1 and S3 share the dc-link voltage equally when they are simultaneously turned OFF, one can obtain

$$V_{1N} = V_{3N} = \frac{V_{\mathrm{dc}}}{2} \tag{5}$$

Therefore, the total Voltage during the freewheeling stage is calculated as

$$V_{t\mathrm{CM}} = \frac{V_{1N} + V_{3N}}{2} + (V_{1N} - V_{3N}) \cdot \frac{L_{o1} - L_{o3}}{2(L_{o1} + L_{o3})} = \frac{V_{\mathrm{dc}}}{2} \tag{6}$$

Equations (4) and (6) indicate that the total CM voltage keeps constant in the whole positive half-line cycle. As a result, no CM current is excited. Similarly, during the whole negative half-line cycle, the CM leakage current mode is exactly the same as the one during the positive half-line cycle; the only difference is the activation of different devices. The total CM voltage in the negative half-line cycle is also equal to *V*dc/2. Therefore, in the whole grid cycle the total CM voltage keeps constant, minimizing CM ground leakage current.

4. PHOTOVOLTAIC (PV) SYSTEM

In the crystalline silicon PV module, the complex physics of the PV cell can be represented by the equivalent electrical circuit shown in Fig. 5. For that equivalent circuit, a set of equations have been derived, based on standard theory, which allows the operation of a single solar cell to be simulated using data from manufacturers or field experiments.

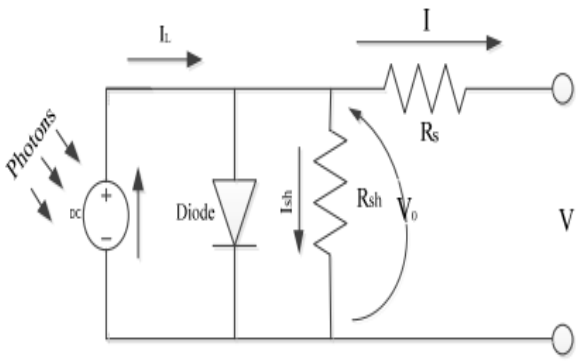

Fig.8 Equivalent electrical circuit of a PV module

The series resistance RS represents the internal losses due to the current flow. Shunt resistance Rsh, in parallel with diode, this corresponds to the leakage current to the ground. The single exponential equation which models a PV cell is extracted from the physics of the PN junction and is widely agreed as echoing the behavior of the PV cell.

$$I = I_L - I_{sc}\left(exp\frac{(V + R_s I)}{V_t} - 1\right) - \frac{(V + R_s I)}{R_{sh}} \quad (7)$$

The number of PV modules connected in parallel and series in PV array are used in expression. The Vt is also defined in terms of the ideality factor of PN junction (n), Boltzmann's constant (KB), temperature of photovoltaic array (T), and the electron charge (q). applied a dynamical electrical array reconfiguration (EAR) strategy on the photovoltaic (PV) generator of a grid-connected PV system based on a plant-oriented configuration, in order to improve its energy production when the operating conditions of the solar panels are different. The EAR strategy is carried out by inserting a controllable switching matrix between the PV generator and the central inverter, which allows the electrical reconnection of the available PV modules.

5. BLDC MODEL

The BLDC motor is an AC synchronous motor with permanent magnets on the rotor (moving part) and windings on the stator (fix part). Permanent magnets create the rotor flux. The energized stator windings create electromagnet poles. The rotor (equivalent to a bar magnet) is attracted by the energized stator phase, generating a rotation. By using the appropriate sequence to supply the stator phases, a rotating field on the stator is created and maintained. This action of the rotor - chasing after the electromagnet poles on the stator - is the fundamental action used in synchronous permanent magnet motors. The lead between the rotor and the rotating field must be controlled to produce torque. This synchronization implies knowledge of the rotor position.

The BLDC Motor Control

The key to effective torque and speed control of a BLDC motor is based on relatively simple torque and Back EMF equations, which are similar to those of the DC motor. The Back EMF magnitude can be written as:

$$E = 2NlrB\omega \quad (8)$$

And the torque term as

$$T = \left(\frac{1}{2}i^2\frac{dL}{d\theta}\right) - \left(\frac{1}{2}B^2\frac{dR}{d\theta}\right) + \left(\frac{4N}{\pi}Brl\pi i\right) \quad (9)$$

Where N is the number of winding turns per phase, l is the length of the rotor, r is the internal radius of the rotor, B is the rotor magnet flux density, ω is the motor's angular velocity, i is the phase current, L is the phase inductance, θ is the rotor position, R is the phase resistance.

6. SIMULATION RESULTS

1) Proposed Inverter Module

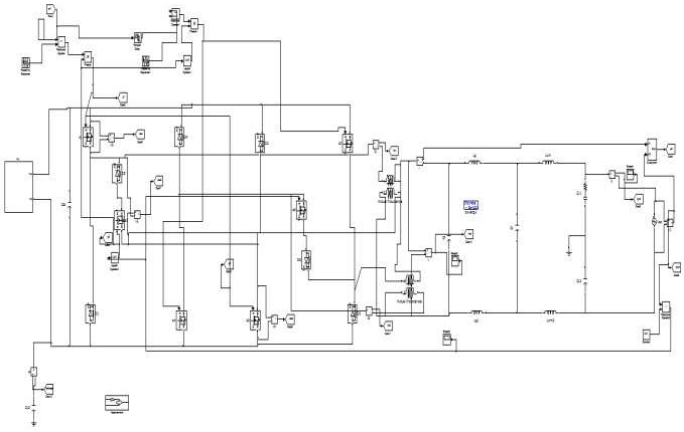

Fig.10 Matlab/simulink model of proposed inverter

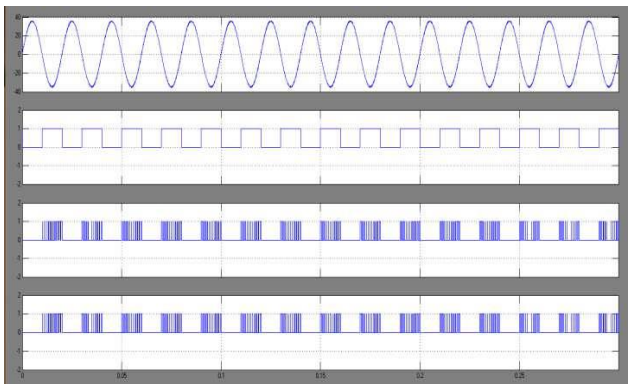

Fig.11 Switch gating signals in grid cycle

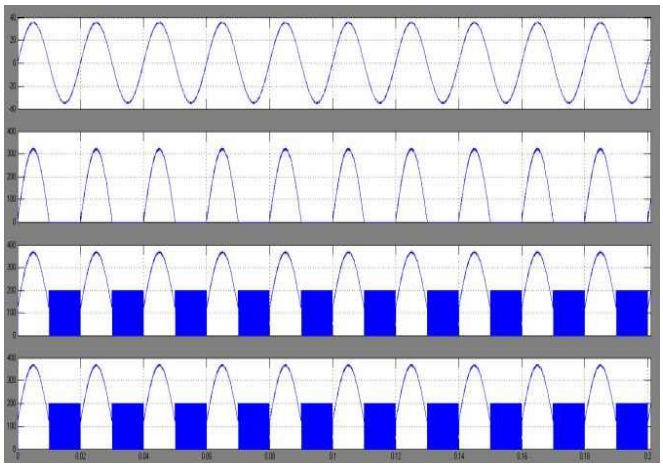

Fig.12 Drain–source voltage waveforms of the switches S1, S3, and S
in grid cycle

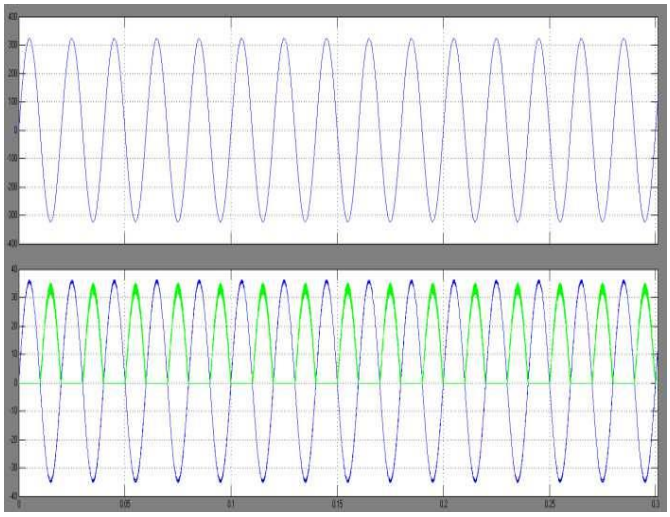

Fig.13 simulated waveforms of ground potential VEN , grid current,
and current of inductor Lo 1

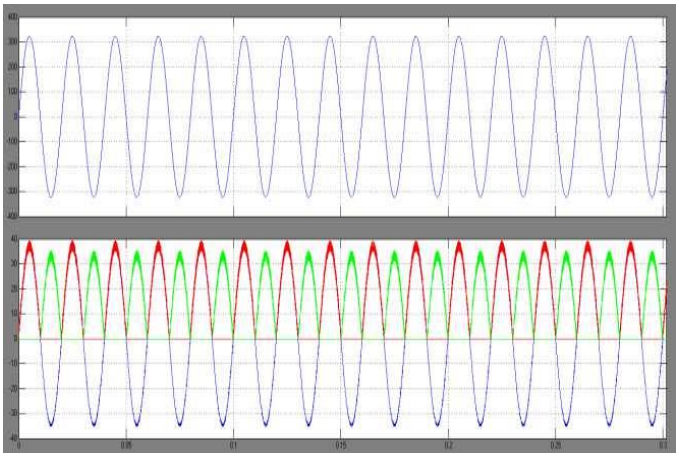

Fig.14 simulated waveforms of grid current and the inductor
Currents iLo1 and iLo2

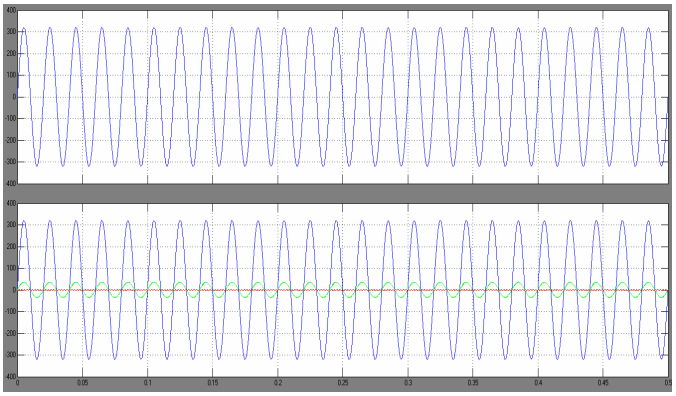

Fig.15 Leakage current test waveforms

Case 2: Application to BLDC Drive System with PV Fed Proposed Inverter Topology.

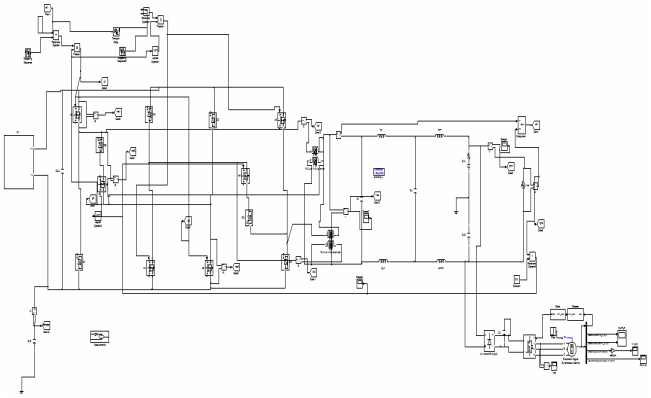

Fig.16 Matlab/Simulink Model of BLDC Drive System with PV Fed Proposed Inverter Topology

Fig.16 shows the Matlab/Simulink Model of BLDC Drive System with PV Fed Proposed Inverter Topology using Matlab/Simulink Platform.

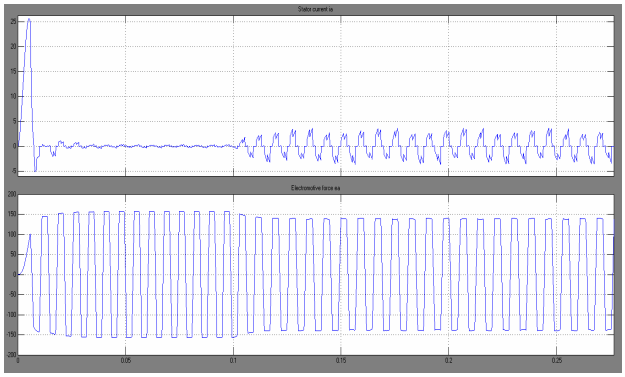

Fig.17 Armature Current, Back EMF

Fig.17 shows the Armature Current, Back EMF of BLDC Drive System with PV Fed Proposed Inverter Topology.

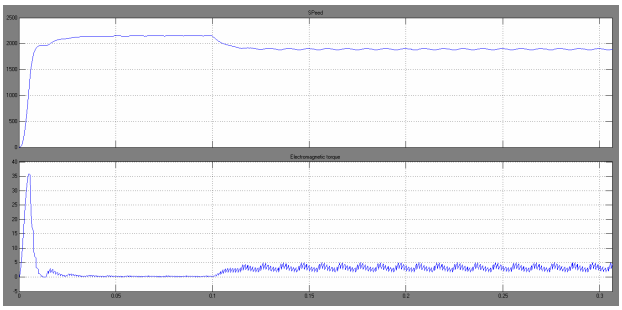

Fig.18 Speed, Electromagnetic Torque

Fig.18 shows the Speed & Electromagnetic Torque of BLDC Drive System with PV Fed Proposed Inverter Topology.

VI. CONCLUSION

BLDC have been used incdifferent applications such as industrial automation, automotive, aerospace instrumentation and appliances since 1970's. This paper has proposed Single phase and Three Phase power conversion system with BLDC drive application. A number of integrated energy systems based on a compact converter topology. A high reliability and efficiency inverter for transformerless PV connected power generation systems with BLDC drive and grid connected system is presented in this paper. Ultra high efficiency can be achieved over a wide output power range by reliably employing super junction MOSFETs for all switches since their body diodes are never activated and no shoot-through issue leads to greatly enhanced reliability. Low ac output current distortion is achieved because dead time is not needed at PWM switching commutation instants and grid-cycle instants. The higher operating frequencies with high efficiency enables reduced cooling requirements and results in system cost savings by shrinking passive components.

REFERENCES

[1] Naman Hariom Agarwal and B. B. Pimple, "Solar photovoltaic array based brushless DC motor for fans in Indian railways using maximum power point tracking algorithm ," *IEEE National Systems Conference (NSC), pp 1-6*, 13 June 2016

[2] Rajan Kumar and Bhim Singh, "Buck boost converter fed BLDCmotor drive for PV array based water pumping," *IEEE International Conference on Power Electronics, Drives and Energy Systems (PEDES)*, pp.1-6, 16-19 Dec. 2014..

[3] Zhou Xuesong, Song Daichun, Ma Youjie and Cheng Deshu,"The simulation and design for MPPT of PV system based on Incremental Conductance method," *2010 WASE International Conference on Information Engineering (ICIE)*, pp.314-317, 14-15 Aug. 2010.

[4] Mohammed A. Elgendy, Bashar Zahawi, and David J. Atkinson, "Assessment of Incremental Conductance maximum power point tracking algorithm," *IEEE Transactions on Sustainable Energy*, vol.4, no.1, Jan. 2013.

[5] J. S. Lai, "Power conditioning circuit topologies," *IEEE Ind. Electron. Mag.*, vol. 3, no. 2, pp. 24–34, Jun. 2009.

[6] S. B. Kjaer, J. K. Pedersen, and F. Blaabjerg, "A review of singlephase grid-connected inverters for photovoltaic modules," *IEEE Trans. Ind. Appl.*, vol. 41, no. 5, pp. 1292–1306, Sep./Oct. 2005.

[7] M. Calais, J.Myrzik, T. Spooner, and V. G. Agelidis, "Inverters for singlephase grid connected photovoltaic systems—An overview," in *Proc. IEEE Annu. Power Electron. Spec. Conf.*, 2002, vol. 2, pp.1995–2000.

[8] Y. Xue, L. Chang, S. B. Kjaer, J. Bordonau, and T. Shimizu, "Topologies of single-phase inverter for small distributed power generators: An overview," *IEEE Trans. Power Electron.*, vol. 19, no. 5, pp. 1305–1314, Sep. 2004.

[9] Q. Li and P.Wolfs, "A review of the single phase photovoltaic module integrated converter topologies with three different DC link configurations," *IEEE Trans. Ind. Electron.*, vol. 23, no. 23, pp. 1320–1333, Apr. 2008.

[10] J. M. A. Myrzik and M. Calais, "String and module integrated inverters for single-phase grid connected photovoltaic systems-A review," in *Proc. IEEE Bologna Power Tech Conf.*, Bologna, Italy, Jun. 2003, pp. 430–437.

[11] F. Schimpf and L. E. Norum, "Grid connected converters for photovoltaic, state of the art, ideas for improvement of transformerless inverters," presented at the Nordic Workshop Power Ind. Electron., Espoo, Finland, Jun. 2008.

[12] R. Gonzalez, J. Lopez, P. Sanchis, and L. Marroyo, "Transformerless inverter for single-phase photovoltaic systems," *IEEE Trans. Power Electron.*, vol. 22, no. 2, pp. 693–697, Mar. 2007.